Simulating the nitrogen migration in Be/W tokamaks with WallDYN

G. Meisl[a], K. Schmid[a], K. Krieger[a,b], M. Oberkofler[a], S.W. Lisgo[c] and JET contributors[b]

[a] **Max-Planck-Institut für Plasmaphysik, Boltzmannstraße 2, 85748 Garching, Germany**

[b] **EUROfusion Consortium, JET, Culham Science Centre, OX14 3DB, Abingdon, UK** ‡

[c] **ITER Organization, FST, Route de Vinon, CS 90 046, 13067 Saint Paul Lez Durance Cedex, France**

E-mail: gmeisl@ipp.mpg.de

Abstract.

The migration of wall material or seeding impurities plays an important role in the formation of mixed materials, the impurity contamination of the plasma and tritium retention. First, this work presents an improved model for the sputtering from mixed material surfaces in WallDYN. Second, we present dynamic SDTrimSP and WallDYN simulations of the nitrogen implantation in Be and the migration of nitrogen in toka-

‡ See the Appendix of F. Romanelli et al., Proceedings of the 25th IAEA Fusion Energy Conference 2014, Saint Petersburg, Russia

maks with a Be main wall. The simulations with the binary collision code SDTrimSP predict that N accumulates directly at the surface and that the Be erosion decreases with increasing N surface content. A first application of WallDYN to the nitrogen migration with an ITER-like wall indicates that the Be main wall may cause wall pumping of N by co-deposition with Be.

PACS numbers: 79.20.Ap, 52.25.Vy, 52.40.Hf, 52.65.-y

1. Introduction

Experiments in ASDEX Upgrade (AUG) and JET have demonstrated the ability to control the power load onto the divertor target plates by N_2 puffing [1, 2, 3]. In contrast to hydrogen and noble gases, N chemically interacts with tungsten and beryllium surfaces. This leads to a storage of nitrogen from the plasma in the wall surfaces. As the surfaces have only a limited N storage capacity, excess N is reemitted from saturated surfaces.

The accumulation and migration of N in tokamaks has already been studied experimentally in AUG [4, 5, 6, 7, 8], TEXTOR [9] and JET [10, 11, 12]. For AUG many of the experimental results could be reproduced by WallDYN simulations employing a novel model for the N saturation [7, 8].

This work employs WallDYN to study the N migration in JET and ITER as examples of devices with a Be main wall. As a first step, the accumulation of N in Be under D-N co-bombardment is studied with SDTrimSP simulations [13]. Then, recent extensions

to the WallDYN model are described which improve the accuracy of the sputter and N-saturation models. Finally, WallDYN predictions on the N accumulation in JET-ILW and ITER are presented. It has to be pointed out, that these simulations cannot yet give a concluding picture of the N migration in JET or ITER, but rather should help to prepare experiments for a detailed benchmarking of WallDYN.

Currently, only few experimental results concerning the N migration in JET-ILW are available: A study of the N retention and legacy with Be main wall, mainly based on residual gas analysis and spectroscopy, was reported in Ref. [11]. A surface analysis of tiles removed from JET reported a rather inhomogeneous distribution of N, with a pronounced maximum in the net-deposition region on the apron above the inner divertor [12].

2. Accumulation of N in Be under D-N co-bombardment

SDTrimSP [13] is widely used to simulate the interaction of energetic ions with matter. It is based on the binary collision approximation in combination with electronic stopping, so that chemical effects are not readily taken into account. However, earlier studies have shown that SDTrimSP with a maximum N concentration for N in Be of 40 % is well suited for the simulation of N implantation in Be [14, 15]. As for the case of W surfaces in Ref. [16], the accumulation of N in Be bombarded with D and N atoms with an impact angle of 40° has been simulated with SDTrimSP for varying N fraction in the beam and various energies. As N ions in fusion plasmas are usually multiply ionized and

therefore have higher impact energies than D ions under the same conditions, the impact energy of the N ions was set to twice the energy of the D ions. For D ion energies in the range from E_D =15–500 eV this results in E_N =30–1000 eV, corresponding to a mean implantation depth of the N projectiles of roughly 2–30 Å [17]. It should be noted that SDTrimSP and WallDYN do not include thermally activated diffusive or chemical effects (apart from enforcing maximum N concentrations). The decomposition of beryllium nitride seems only to set in above 1000 K [14]. The formation of tungsten nitride is suppressed already at significantly lower temperatures [16], however, quantitative models for the temperature dependence of WN formation decomposition are not yet available. Temperature effects could be important especially for the divertor surfaces in ITER, where surface temperatures above 1000 K are expected.

Figure 1 shows exemplarily the N depth profiles simulated with SDTrimSP for bombarding a Be surface with 92 % D and 8 % N. With increasing energy the implantation depth and the N content increase. Different from the case of W surfaces with a N peak in a few nm depth [16], the maximum N concentration develops on the surface. Furthermore, simulations on the bombardment of Be surfaces with a mixture of D+N+Be (not shown here) indicate that the N/Be ratio in deposited layers does not reach the ratio of stoichiometric Be_3N_2.

Figure 2 shows that for all considered impact conditions the N saturation areal density increases with increasing implantation energy. With increasing D fraction in the beam the N areal density decreases, because the D leads to an enhanced N re-erosion. Figure

2 also includes results from the WallDYN model, which are discussed in section 3. In this section also sputtering of Be under D-N bombardment is discussed. It should be noted that the sputter and reflection yield in WallDYN are calculated from fits to static SDTrimSP calculations. Still, deviations between WallDYN and SDTrimSP can arise from depth profile effects, as WallDYN assumes a homogeneous composition of the surface.

3. WallDYN model and recent improvements

To include the complete migration chain of erosion, transport through the plasma, re-deposition and potential re-erosion in our analysis, we employ the WallDYN code [8, 18] for our analysis of the N migration. WallDYN simulates the evolution of the surface composition of the first wall, which is discretized into about 50 poloidally distributed wall tiles. The plasma-wall interaction module of WallDYN includes physical sputtering and reflection based on SDTrimSP calculations. The transport of impurities in the plasma is calculated with DIVIMP [19]. An important input for WallDYN and DIVIMP is the plasma background, i.e. spatially resolved data on the plasma density, temperature and flow velocity.

The plasma background employed for the ITER simulations is based on a SOLPS simulation of a medium density H-mode (P_{SOL}=100 MW, scenario *i-ref-0003-1514-00o*) plasma. Relatively small Mach number in Fig. 3 indicate rather weak SOL flows. To improve the accuracy of the plasma-wall interaction in the main wall region, the plasma was extrapolated from the SOLPS grid to the main wall with the onion-skin model as

described in Ref. [20]. For the JET simulations the plasma background for the low density ohmic shot of Ref. [21] was employed. For the perpendicular transport of impurities a constant anomalous diffusion coefficient of $D_\perp = 1\ m^2 s^{-1}$ was used. It should be noted, that the plasma backgrounds do not include the effect of nitrogen seeding on the plasma. The JET OSM solution represents a pure D plasma, the SOLPS plasma for ITER consists of D as main species and small amounts of He and C.

The loss of N to the vacuum pumping system is modeled by pumping tiles (green lines in Fig. 3) with zero sputter and reflection yield. As described in Ref. [8], a model to reproduce the N saturation in W has recently been included in WallDYN. For the present work, this model was extended to include the energy dependence of the N saturation areal density (σ_{Sat}) in Be. Based on the SDTrimSP simulations presented in the previous section the employed N saturation areal density is:

$$\sigma_{Sat} = \left(0.25 + 0.003 \cdot \frac{2\,T_i + 3\,T_e}{\mathrm{eV}}\right) 10^{20}\,\mathrm{N/m^2} \tag{1}$$

Figure 2 gives a direct comparison of SDTrimSP simulations to results from WallDYN. It should be noted that the reflection and sputter yields in WallDYN are calculated from fits to static SDTrimSP simulations. Still, deviations between SDTrimSP and WallDYN arise because WallDYN does not take into account the effects arising from the elemental depth distribution. The dark green dotted curve is based on the WallDYN surface model without a maximum areal density. In contradiction to the experimental results this curve rises continuously. The WallDYN results using the energy dependent

σ_{Sat} (dotted and dashed curves) largely agree with SDTrimSP. The only notable exception is the WallDYN simulation for 3 % N and E_D=250 eV. While there is a slight decrease in the saturation N areal density with decreasing N fraction in all WallDYN simulations, the strong N re-erosion for this special case is not reproduced by WallDYN. The reason for this discrepancy is the assumption of a homogeneous surface layer in WallDYN. Because the real N depth profile is peaked towards the surface, the real N re-erosion is higher than predicted by WallDYN§.

In WallDYN the wall surfaces are modeled by a reaction zone of a 4 nm thickness and a bulk zone [18]. Material is exchanged between these two zones to keep the thickness (more specifically the areal density) of the reaction zone constant. The saturation model limits the areal density in the reaction zone, but under net deposition conditions material is transported from the reaction zone to the bulk zone. By this mechanism the total N areal density may rise above the specified maximum areal density, reflecting the process of co-deposition of N with other elements like Be. With a maximum N areal density of around $0.4 \cdot 10^{20} N/m^2$ and typical 'thicknesses' of reaction zones in WallDYN of around $4 \cdot 10^{20} \#/m^2$, the N/Be ratio in the reaction zones and therefore also in the bulk fluxes is in the range of 0–0.1. This range is in agreement with the range of N/Be ratios in Be-N co-deposits reported from PISCES-B experiments [22, 23].

§ For N in W it is just the other way round and WallDYN seems to overestimate the N erosion [8]

3.1. Sputtering of mixed materials

As described in Ref. [18] the sputter yield of species e from a mixed material surface in WallDYN is usually calculated by

$$Y^e_{sput} = \frac{\sigma_e}{\sigma_{tot}} \cdot Q_0 \cdot Y_{Bohdansky}(E_{Kin}, E_{Thresh}) \cdot \left(1 + \sum_{i=1}^{N} a_i \sigma_i\right) \tag{2}$$

where E_{Kin} is the kinetic energy of the impinging particle, σ_i is the areal density and σ_i/σ_{tot} the concentration of species i in the target surface, N the number of elements, and the parameters Q_0, E_{Thresh} and a_i are determined individually for each projectile-target combination by a fit to SDTrimSP simulations. This formula works well in that it generally reproduces the known energy dependence of the sputter yield and includes effects of the composition on the sputter yield. A technical problem related to this formula is the interdependency of the parameters Q_0 and a_e. This makes it rather difficult to compare different sets of these parameters or to compare such parameters to experimental results.

To overcome this problem a modified expression for the sputter yield was introduced in WallDYN:

$$Y^e_{sput} = \frac{\sigma_e}{\sigma_{tot}} \cdot Q_0^{pure} \cdot Y_{Bohdansky}(E_{Kin}, \tilde{E}_{Thresh}) \cdot \left(1 + a_e \left(1 - \frac{\sigma_e}{\sigma_{tot}}\right)\right) \cdot \prod_{i \neq e}^{N} \left(1 + a_i \frac{\sigma_i}{\sigma_{tot}}\right); \quad a_i > -1 \tag{3}$$

where Q_0^{pure} is fitted to SDTrimSP simulations with $\sigma_e/\sigma_{tot} = 1$ and can be easily compared to experimental results. A composition dependence is introduced by the terms a_i and by $\tilde{E}_{Thresh}$

$$\tilde{E}_{Thresh} = E^{pure}_{Thresh} \cdot \left(1 + b_e \left(1 - \frac{\sigma_e}{\sigma_{tot}}\right)\right) \cdot \prod_{i \neq e}^{N} \left(1 + b_i \frac{\sigma_i}{\sigma_{tot}}\right); \qquad b_i > -1 \tag{4}$$

which is composed of E_{Thresh}^{pure}, the threshold energy for a pure elemental surface with $\sigma_e/\sigma_{tot} = 1$, and a term representing the composition dependence of the threshold energy. This model for the sputtering from mixed surfaces avoids the problems associated with the interdependency of Q_0 and a_e, but also results in a better quality of the fits.

Figure 4 shows the evolution of the Be sputter yield under D-N bombardment from SDTrimSP and WallDYN simulations. The sputter yields for pure Be agree very well. Also both codes predict a decrease of the Be sputter yield due to N accumulation in the surface with increasing fluence‖. The magnitude of this decline depends on the enrichment of N at the surface, and is therefore smaller in WallDYN than in SDTrimSP.

4. Application of WallDYN to the N migration in tokamaks with Be main wall

Similar to the WallDYN predictions for AUG, N starts to accumulate in the surfaces close to the injection location and in the divertor. The N areal density predicted for 15 s with the ITER geometry and a N puff of $1.43 \cdot 10^{22} \frac{\mathrm{N}}{\mathrm{s}}$ ¶ from the divertor is shown in Fig. 3. One can see that N is present in the whole divertor region and in large parts of the main wall. The dark areas of the wall represent regions, where the N areal density significantly exceeds the N saturation areal density specified for the reaction zone. These areas are regions of net Be deposition and the comparatively high N areal densities result from

‖ In contrast, SDTrimSP predicts that the W sputter yield under D-N bombardment is constant [16]

¶ Corresponding to a very strong N puff in JET

a "co-deposition" of N with Be. SOL flows to the high field side, as they are usually observed experimentally [24], would shift the Be deposition areas, and therefore the N co-deposition, to the high field side.

This is actually the case for the JET simulations, which are based on a plasma background featuring strong SOL flows towards the high field side. In these simulations the co-deposition of N with Be is predicted to occur on the apron above the inner divertor, similar to the results from Ref. [12]. For the long term N balance the co-deposition of N with Be leads to a continuous increase of the N wall inventory, different from the case of AUG with a W main wall. As an estimate for the wall inventory in JET after puffing $3.8 \cdot 10^{22}$ N atoms the simulation gives a value of $0.9 \cdot 10^{22}$ N atoms. This value has to be compared to $2 \cdot 10^{22}$ N atoms, which were missing in the gas balance in Ref. [11]. Taking into account that part of the missing N probably sticks in the vessel in the form of ammonia (a process not included in WallDYN) and the uncertainties entering the calculation of this number, this seems like a reasonable agreement.

Finally, we want to discuss the impact of the plasma wall interaction on the N fluxes and distribution in the plasma. To this end Fig. 5 shows the results from 4 WallDYN simulations with an ITER geometry. These simulations differ in the location of the N puff, which is either in the divertor or from the vessel top, and in the magnitude of the sputter and reflection yields, which are based either on simulations with perpendicular impact or an impact angle of 40°. In Fig. 5a one can see the evolution of the effective N fluxes into the plasma. For the simulations with N puff from the top, the initial flux is not

increased above the the puff rate, because the kinetic reflection yield for N ions impinging on the Be surfaces around the puff location is very low. For the simulations with divertor puff, the total N flux into the plasma at $t = 0$ s is increased by the kinetic reflection of N impinging on W surfaces to $1.9 \cdot 10^{22} \frac{\mathrm{N}}{\mathrm{s}}$ and $2.2 \cdot 10^{22} \frac{\mathrm{N}}{\mathrm{s}}$ for the case employing the yields for perpendicular impact and an impact angle of 40°, respectively. As the surfaces get saturated with N, the effective N reflection coefficient and the N flux into the plasma rise by more than two orders of magnitude. Thereby, the N flux is higher for a puff from the vessel top (further away from the pumping system) and lower for the simulations with higher sputter yield (which leads to stronger wall pumping by co-deposition). Figure 5b shows the ratio of N fluxes to the outer divertor target to the N core concentration as a measure for the divertor enrichment. For the N puff from the vessel top the wall pumping reduces the divertor enrichment and so the saturation of the surface N content increases the divertor enrichment. For the N puff from the divertor, less N is transported into the main plasma with stronger wall pumping. That means the divertor enrichment goes down with increasing N surface coverage or smaller sputter yields. Still, WallDYN predicts that the divertor enrichment for the case of a divertor puff remains higher than the enrichment for a puff from the vessel top.

5. Conclusion

This work is part of an effort to improve the understanding of N migration by combining laboratory experiments, computer simulations and tokamak experiments [7, 8, 16]. The

present contribution extends this study to tokamaks with a Be main wall. To get a better insight into the interaction of energetic N with a plasma exposed Be surface, SDTrimSP simulations have been performed. These simulations result in N depth profiles, where the N concentration steadily decreases with increasing depth and where the N saturation areal density increases with implantation energy. However, as experimental studies on the interaction of N with Be are scarce, significant uncertainties remain, especially with respect to processes like chemical erosion of N from Be [23], the diffusion of N in Be or the co-deposition of N with Be .

Based on the results from SDTrimSP, an energy dependent N saturation areal density has been introduced to describe the interaction of N with Be in WallDYN. Additionally, an improved model for the physical sputtering of mixed material surfaces has been included in WallDYN. According to the WallDYN simulations N becomes stored in the divertor and main wall surfaces and the co-deposition of N with Be may lead to comparatively large N areal densities in net-deposition areas.

6. Acknowledgments

This work has been carried out within the framework of the EUROfusion Consortium and has received funding from the Euratom research and training programme 2014-2018 under grant agreement No 633053. The views and opinions expressed herein do not necessarily reflect those of the European Commission. This work was done under EUROfusion WP PFC.

[1] A. Kallenbach, M. Balden, et al., *J. Nucl. Mater 415, S19 (2011)*, http://dx.doi.org/10.1016/j.jnucmat.2010.11.105

[2] F. Reimold, M. Wischmeier, et al., *J. Nucl. Mater. in Press*, http://dx.doi.org/10.1016/j.jnucmat.2014.12.019

[3] M. Wischmeier, The ASDEX Upgrade team and JET EFDA contributors, *J. Nucl. Mater. in Press*, http://dx.doi.org/10.1016/j.jnucmat.2014.12.078

[4] A. Kallenbach, R. Dux, et al., *Plasma Phys. Control. Fusion 52 055002 (2010)*, dx.doi.org/10.1088/0741-3335/52/5/055002

[5] D. Neuwirth, V. Rohde, et al., *Plasma Phys. Control. Fusion 54 085008 (2012)*, http://dx.doi.org/10.1088/0741-3335/54/8/085008

[6] P. Petersson, A. Hakola, et al., *J. Nucl. Mater. 438, S616 (2013)*, http://dx.doi.org/10.1016/j.jnucmat.2013.01.129

[7] G. Meisl, K. Schmid, et al., *J. Nucl. Mater. (2014), in Press*, http://dx.doi.org/10.1016/j.jnucmat.2014.10.031

[8] G. Meisl, K. Schmid, et al., Experimental analysis and WallDYN simulations of the global nitrogen migration in ASDEX Upgrade L-mode discharges, *submitted to Nuclear Fusion*

[9] M. Rubel, V. Philipps, et al. *J. Nucl. Mater. 415, S223 (2011)*, http://dx.doi.org/10.1016/j.jnucmat.2010.08.035

[10] S. Brezinsek, T. Loarer, et al., *Nucl. Fusion 51, 073007 (2011)*, http://dx.doi.org/10.1088/0029-5515/51/7/073007

[11] M. Oberkofler, D. Douai, et al., *J. Nucl. Mater 438, S258* (2013), http://dx.doi.org/10.1016/j.jnucmat.2013.01.041

[12] P. Petersson , M. Rubel, et al., *J. Nucl. Mater., in Press*, http://dx.doi.org/10.1016/j.jnucmat.2014.12.077

[13] A. Mutzke, R. Schneider, et al., *IPP Report 12/08, Max-Planck-Institut für Plasmaphysik (Hrsg.)*

(2011)

[14] M. Oberkofler, and Ch. Linsmeier, *Nucl. Fusion 50, 125001 (2010)*, http://dx.doi.org/10.1088/0029-5515/50/12/125001

[15] K. Dobes, M. Köppen, M. Oberkofler, et al., *NIMB 340, 34 (2014)*, http://dx.doi.org/10.1016/j.nimb.2014.06.025

[16] G. Meisl, K. Schmid, et al., *New J. Phys. 16, 093018 (2014)*, http://dx.doi.org/10.1088/1367-2630/16/9/093018

[17] W. Eckstein, *IPP Report 17/20, Max-Planck-Institut für Plasmaphysik (Hrsg.) (2010)*, http://edoc.mpg.de/display.epl?mode=doc&id=476831&col=33&grp=1311#cb

[18] K. Schmid, M. Reinelt, and K. Krieger, *J. Nucl. Mater. 415, S284 (2011)*, http://dx.doi.org/10.1016/j.jnucmat.2011.01.105

[19] P.C. Stangeby, J.D. Elder, *J. Nucl. Mater 196, 258 (1992)*, http://dx.doi.org/10.1016/S0022-3115(06)80042-5

[20] S.W. Lisgo, A. Kukushkin, et al., *J. Nucl. Mater. 438, S580 (2013)*, http://dx.doi.org/10.1016/j.jnucmat.2013.01.121

[21] K. Schmid, K. Krieger, et al., *J. Nucl. Mater., in Press*, http://dx.doi.org/10.1016/j.jnucmat.2014.11.109

[22] M. Oberkofler, G. Meisl, et al., *This conference*

[23] T. Dittmar, M.J. Baldwin, et al., *Phys. Scr. T145, 014009 (2011)*, http://dx.doi.org/10.1088/0031-8949/2011/T145/014009

[24] G.F. Matthew, *J. Nucl. Mater. 337, 1 (2005)*, http://dx.doi.org/10.1016/j.jnucmat.2004.10.075

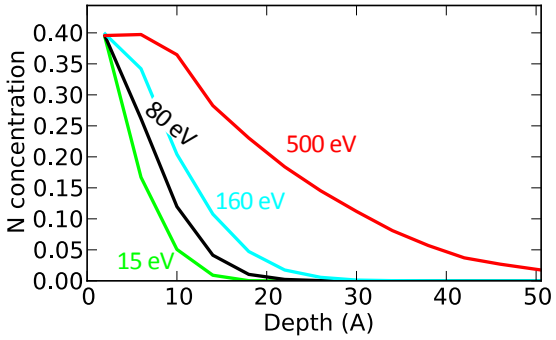

Figure 1. Steady state N depth profiles in a Be surface under bombardment with 92% D and 8% N, E_N=2 E_D.

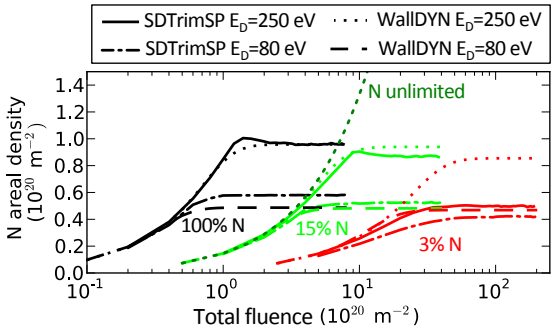

Figure 2. Accumulation of N in Be surface as function of the D+N fluence calculated with SDTrimSP and the WallDYN model. N has twice the energy of D. The color indicates the fraction of N in the incoming beam. For 15 % N also a simulation with the WallDYN model without saturation model is shown. The N areal density increases with increasing energy and increasing N fraction.

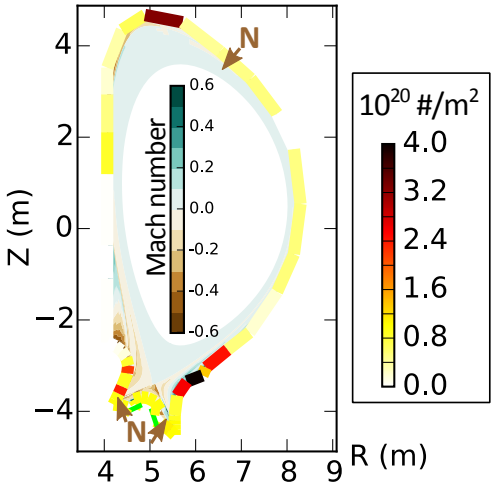

Figure 3. Wall configuration and background plasma flows for ITER simulations: N is puffed either from two locations in the divertor or from the vessel top. The color of the wall tiles represents the N areal density after 15 s for the simulation with N puff from the divertor and yields calculated for 40° impact angle. In net deposition areas the N areal density exceeds the specified saturation areal density. The plasma background exhibits only weak flows in the SOL.

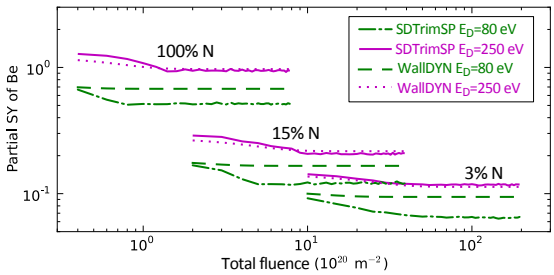

Figure 4. Partial sputter yield (i.e. number of sputtered Be atoms per impinging projectile) evolution of Be as function of the D+N fluence with $E_N = 2E_D$ calculated with SDTrimSP and WallDYN. The sputter yield decreases with decreasing N fraction in the beam and with fluence, as N accumulates in the surface.

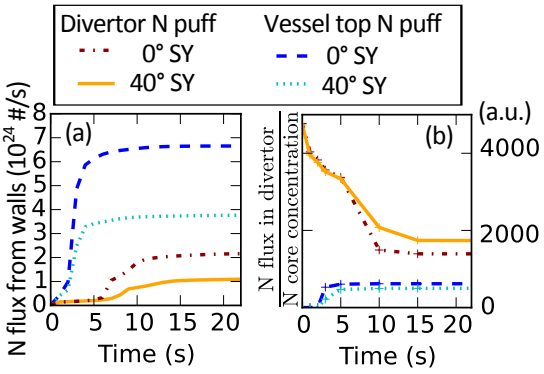

Figure 5. WallDYN simulations on the impact of the plasma-wall interaction on N fluxes and distribution in the plasma of ITER. (a) shows the evolution of the N flux into the plasma, which is of the order of the N puff rate ($1.43–2.2 \cdot 10^{22} \frac{\mathrm{N}}{\mathrm{s}}$) for t=0 and rises by about a factor of 100 as N recycling gets more effective with increasing N wall coverage. (b) predicts that the divertor enrichment of N strongly depends on the surface conditions and is stronger for a N source in the divertor.